

Performance assessment of existing models to predict brittle failure modes of steel-to-timber connections loaded parallel-to-grain with dowel-type fasteners[☆]

J. M. Cabrero^{a,*}, M. Yurrita^a

^aWood Chair. Department of Building Construction, Services and Structures. University of Navarra. 31009 Pamplona (Spain)

Abstract

For safety reasons, ductile failure in timber connections with dowel-type fasteners is always recommended. It has usually been assumed that it can be achieved by fulfilling minimum spacing requirements between fasteners. However, recent works address the need to account for brittle failure modes (namely splitting, row-shear, and block and plug-shear) in connections loaded parallel-to-the-grain in an explicit manner, in order to evaluate them and achieve the desired ductility. This article describes the brittle failure modes and reviews the existing calculation models proposed by several authors -some of them included in standards-. Finally, the performance of these models is assessed against an extensive database of tests gathered from the literature following a comprehensive methodology.

Keywords:

Brittle failure parallel-to-grain, Splitting, Row-shear failure, Block-shear failure, Plug-shear failure, Timber connections

1. Introduction

It is well known that connections are of crucial importance in the behaviour of a structure, not only in terms of cost or influence on the global structural behaviour, but also in terms of safety. They have been reported to be involved in almost one quarter of recent collapses of timber structures, where more than half of the involved connections were with dowel-type fasteners [1, 2].

[☆]This article has been published in Engineering Structures.

Please refer it as: J.M. Cabrero, M. Yurrita, Performance assessment of existing models to predict brittle failure modes of steel-to-timber connections loaded parallel-to-grain with dowel-type fasteners, Engineering Structures, Volume 171, 2018, Pages 895-910, ISSN 0141-0296, <https://doi.org/10.1016/j.engstruct.2018.03.037>

*Corresponding author

Email addresses: jcabrero@unav.es (J. M. Cabrero), myurrital@alumni.unav.es (M. Yurrita)

7 The European Yield Model, included in the Eurocode 5 [3] dates back to early
8 works by Johansen [4] and only provides the capacity for the ductile failure mode of
9 joints, which is governed by the embedment of the timber or the bending of the dowel-
10 type fasteners. It is assumed that no brittle failure occurs if the given minimum spacing
11 requirements are met.

12 However, connections in construction practice include a number of fasteners larger
13 than those currently investigated in the laboratories. As a consequence, the joint ca-
14 pacity could be governed by a brittle failure mode [5]. Nevertheless, designers are not
15 aware of this fact, as shown by a survey conducted in the European area by the Working
16 Group 3 of the COST Action FP1402 [6, 7]: more than 30% of the participants (de-
17 signers, engineers, constructors. . .) did not know about their existence (even up to 24%
18 among those with more than 10 years of experience in the field of timber structures).

19 Some well-known building collapses were originated by a brittle failure of the con-
20 nections, as the Siemens Arena and the Jyväskylä Fair roof [1, 8]. In the case of the
21 Utopia pavilion [5], a previous experimental campaign pointed out the resulting brittle
22 failure, and collapse was prevented at the cost of reinforcing the connections on-site
23 with glued-in-rods.

24 The prenormative version of the Eurocode [9] had been used in both the Jyväskylä
25 Fair roof [8] and the Utopia pavilion [5]. It was demonstrated that it did not cover brittle
26 failure in an adequate way [10, 5]. Those experiences gave rise to a brief description in
27 Racher [11], and a proposal from Ranta-Maunus and Kevarinmäki [10] of a supplement
28 to the Eurocode 5 concerning the calculation of block shear failure. Both stand as the
29 origin of the current Annex A of the Eurocode 5 [3].

30 Brittle failure modes had until then been grouped under the so-called group effect
31 concept [12], which assumed that an interaction effect among the fasteners exists, and
32 as a result the total capacity of the connection is reduced [13]. Nozynski [14], in 1980,
33 was one of the first authors to notice fracture of wood along the row of nails, and
34 proposed the introduction of an effective number of fasteners. Several similar design
35 equations were suggested during the development of the Eurocode 5 [15–17], and were
36 soon adopted by different countries in their design standards [18].

37 However, Smith and Steck [19] noticed already in 1985 the need for new theories
38 to obtain the "*ultimate capacities of joints with brittle failures*". Since then, several ref-
39 erences introduced the concept of brittle failure. Among them, the STEP books, where
40 Racher [11] provides a brief explanation of this concept for dowelled connections, and
41 Kevarinmäki [20] describes it for nailed connections in trusses.

42 Several model proposals for the different types of brittle failure have been made:
43 for splitting [3, 21, 22], row-shear [23, 22] block-shear models for dowelled [23, 24],
44 nailed [25, 26] and riveted connections [27–33]; some of them are fracture-mechanics
45 based models, mainly for splitting and row-shear [34, 16, 35–37]. Most of them will
46 be reviewed in this paper.

47 Brittle failures, such as block and row-shear models were introduced in the early
48 2000s in the Canadian Code O86 [38, 24, 39–42]. In the case of the Eurocode 5 [3],
49 splitting and row-shear failures are implicitly taken into account by means of the effec-
50 tive number of fasteners based on the work by Jorissen [16]. A model for block and
51 plug-shear is included as Annex A [3], dating back to the previously referred proposals
52 [11, 10]. Currently, the subject is under consideration in the New Zealand Standard

53 draft [43] and in the future Eurocode 5. Within the COST Action FP 1402 [7], which
54 aims to prepare background documents for the future Eurocode 5, Working Group 3
55 has been in charge of the review of the different proposals for this type of failure, which
56 this article summarizes.

57 This work provides insight into the different brittle failure modes of steel-to-timber
58 connections with dowel-type fasteners loaded parallel-to-grain. It compiles the differ-
59 ent available models in an ordered and coherent way, and benchmarks them against
60 experimental tests compiled from the literature.

61 Special attention is given to those models which aim at providing a complete and
62 consistent set of equations to discriminate among ductile and brittle failures. Such a
63 complete method is nowadays provided in the New Zealand Standard draft [43], and
64 the method for dowelled connections by Hanhijärvi and Kevarinmäki [44, 22]. It may
65 be argued that also a complete model is given in the Eurocode 5 [3], although some
66 failure modes are implicitly taken into account.

67 The paper is organised as follows: first, the different failure modes and parameters
68 of connections loaded parallel-to-grain are described in Section 2. Section 3 reviews
69 the different existing models for each failure mode. Section 4 provides information
70 about the experimental data set, and the methodology used to compare and benchmark
71 the different models. Special attention is given to the different possible metrics to
72 assess the performance of the models. The results concerning the prediction ability
73 and reliability will be discussed in Section 5.

74 **2. Brittle failure modes in connections loaded parallel-to-the-grain**

75 *2.1. Geometry and types of connections loaded parallel-to-the-grain*

76 Connections with dowel-type fasteners loaded parallel-to-grain (as shown in Fig-
77 ure 1) are often made by means of different types of fasteners e.g. nails, dowels, bolts,
78 (self-tapping) screws. Their number in a connection greatly depends on the type of
79 fastener used, i.e. small diameter fasteners like nails or rivets are often used with a
80 larger quantity within one connection. Only connections made in combination with
81 steel plates are dealt with in this paper. All the different connection configurations con-
82 sidered here are shown in Figure 2. Since the different models give the capacity per
83 shear plane or wood member, the number of shear planes n_s and wood members n_w for
84 each configuration are given in Figure 2 as well.

85 The geometrical parameters and denotations of a typical steel-timber connection
86 with dowel-type fasteners loaded parallel-to-grain are given in Figure 1. This nomen-
87 clature will be used in this paper, and all the model equations will be rewritten accord-
88 ingly.

89 The dimension of the timber member is defined by its width b and thickness t . The
90 relevant connection parameters are mainly related to the spacing of the fasteners in
91 the parallel a_1 and perpendicular a_2 to-the-grain directions, which are usually defined
92 in relation to the fastener diameter d . The edge distances are named a_3 for the end-
93 distance in the parallel direction, and a_4 in the perpendicular direction. These distances
94 have been usually considered a requirement to achieve the desired ductile failure mode
95 [3].

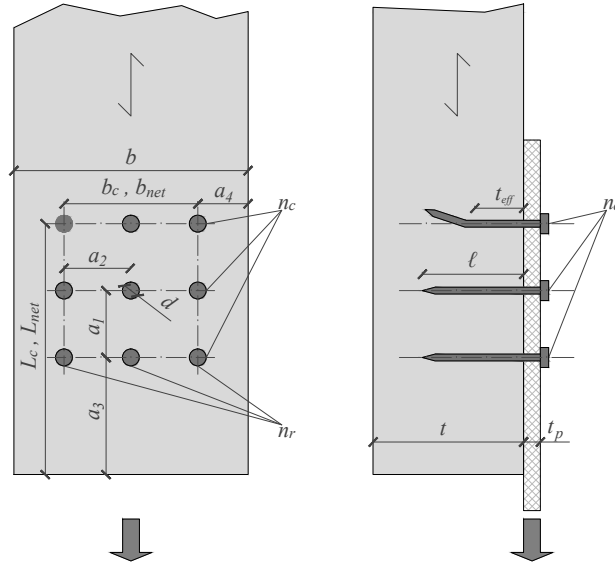


Figure 1: Denotation of connection geometrical parameters used in this paper, depicted for the case of a wood-steel WS connection with small diameter fasteners, as shown in Figure 2a.

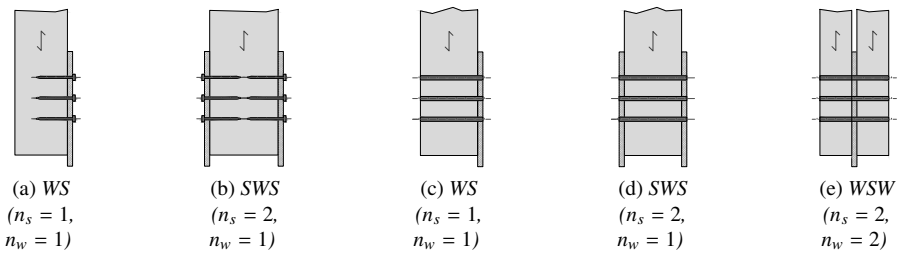


Figure 2: Joint configurations of steel-timber connections: small fasteners (a) and (b), and large fasteners (c)-(e). S= steel, W= wood; n_s = number of shear planes, n_w = number of wood members.

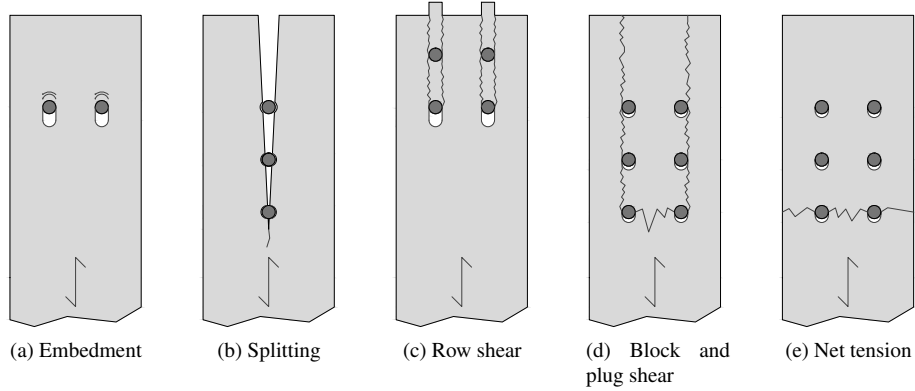


Figure 3: Different possible failure modes of connections loaded parallel-to-grain. Embedment (a) is the only ductile failure mode, the rest are brittle.

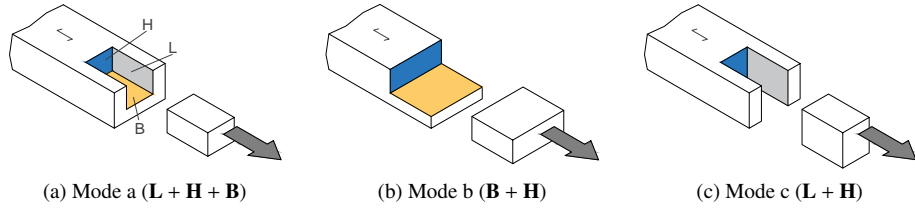


Figure 4: Different possible failure modes of group tear-out.

96 The connection area can be defined by its length L_c and width b_c , where $L_c =$
 97 $a_1 (n_c - 1) + a_3$ and $b_c = b - 2a_4 = (n_r - 1) a_2$. Additionally, the net length, $L_{net} =$
 98 $L_c - (n_c - \frac{1}{2}) d$, and width, $b_{net} = b_c - (n_r - 1) d$, account for the actual dimensions by
 99 deducing the corresponding areas of the fastener holes.

100 **2.2. Failure modes parallel-to-grain**

101 Typical failure modes for connections with dowel-type fasteners loaded parallel-
 102 to-grain are shown in Figure 3, as originally described by Fahlbusch [12]. Embedment
 103 (Fig. 3a) is the only one considered to be ductile, as it is based on plastic deformation of
 104 both wood and steel fasteners. It is the failure mode described by the European Yield
 105 Model (EYM, the Eurocode 5 [3] model), and it therefore is the desired failure mode.
 106 It has usually been assumed that it can be achieved by means of adequate spacing a_i
 107 among the fasteners.

108 The remaining four failure modes in Figure 3 are all brittle. In splitting (Fig. 3b), a
 109 central longitudinal crack forms along the row of fasteners, and it is usually considered
 110 to be related to tension perpendicular to the grain.

111 Row-shear (Fig. 3c) is also produced along the row of fasteners, but it consists on
 112 two parallel cracks instead of one. It is formed by the stresses in shear and in tension

113 perpendicular-to-the-grain, and crack location is related to the location of the maximum
114 shear stress in the vicinity of the hole.

115 Block and plug shear failures (sometimes called group tear-out, Fig. 3d) consist on
116 the tearing out of timber in the connection area. They can be described as the failure
117 of three different planes, as shown in Figure 4, which will be referred throughout this
118 paper as tensile plane **H**, lateral shear planes **L** and bottom shear plane **B**. Different
119 failure modes may happen, depending on the combination of failed planes, as depicted
120 in Fig. 4. Block-shear is usually referred only to connections with large-diameter fas-
121 teners which protrude the whole timber member, and in which the bottom plane **B** is
122 not activated (Fig. 4c). In the case of connections with small-diameter fasteners, which
123 do not protrude the whole thickness, this failure mode is usually called plug-shear, and
124 the bottom-plane is part of the failure as well (Figs. 4b and 4a).

125 Tension failure (Fig. 3e) is already covered in the codes, and it is determined by the
126 capacity of the net area of the wood member, $b_{net} \times t$. It is not considered in this work.

127 Any connection may finally end up failing in a brittle manner at its ultimate capacity
128 [45]. However, for a ductile failure to happen, it would be desirable that the brittle
129 failure would occur after fastener yielding, and thus achieving enough ductility. To
130 that mean, the brittle failure capacity of the connection should be higher than both the
131 fastener yielding and ultimate resistance, in order to avoid brittle and mixed failure
132 modes. The different types of failure and their ranges are described and discussed in
133 detail in [46, 30].

134 **3. Design models for brittle failure of connections loaded parallel-to-grain**

135 The different model proposals for brittle failure in the parallel-to-grain direction are
136 summarized in this Section, grouped by the failure mode they describe.

137 Only the New Zealand Standard draft [43] and the proposal from Hanhijärvi and
138 Kevarinmäki [22] provide a consistent set of equations to deal with all the brittle failure
139 modes at once. The Eurocode 5 [3] covers block-shear in its Annex A. It does not
140 have an explicit model for splitting and row-shear. However, the effective number of
141 fasteners derives from a model which accounted for splitting and shear [16], so it may
142 be assumed that splitting and row-shear failures are implicitly taken into account in this
143 reduction factor.

144 All the equations have been rewritten according to the nomenclature given in Fig-
145 ure 1. The relevant equations are described in each corresponding mode, although in
146 some cases that might be not completely correct according to the complete model.

147 A particular remark must be made for the model of Hanhijärvi and Kevarinmäki
148 [22]. It provides formulae to account for the capacity of the inner and outer parts
149 of the connection, and the total capacity of the connection is obtained as the sum of
150 both. Although provided, they do not describe equations for each failure mode in the
151 same way as this paper does. Therefore, equations shown herein are derived from their
152 proposal. They additionally consider a reduction in the capacity of the planes failing by
153 shear and tension due to the interaction between parallel-to-grain tension, parallel-to-
154 grain shear and perpendicular-to-grain tension stress components. As shown in Sjödin
155 and Johansson [47], highly stressed areas under different stresses overlap, and they

Table 1: Proposals for splitting of connections loaded in the parallel-to-grain direction. Shown strength refers to the capacity of the timber member, with exception of the Eurocode 5, where the reduction factor to be applied to the number of fasteners to obtain the capacity of the connection is given.

Reference	Strength	β_p	Remarks
Literature			
Jorissen [16]	$2t \sqrt{\frac{G_f E_0 d \sin \alpha (b-d \sin \alpha)}{b}}$		
Hanhijärvi and Kevarinmäki [22]	$\begin{cases} \frac{k_{conc}}{\beta_p} \frac{1}{s_{90,hole}} a_3 t f_{t,90} \text{ (hole)} \\ \frac{k_{conc}}{\beta_p} \frac{1}{s_{90,end}} a_3 t f_{t,90} \text{ (end)} \end{cases}$	$\frac{1}{10}$	Different beginning locations. $s_{90,i}$ are geometric parameters. $k_{conc} = 0.7$
Jockwer et al. [48]	$2\beta_p t a_3 f_{t,90}$	$\frac{1}{7}$	
Standards			
Eurocode 5 [3]	$n_{ef} = \begin{cases} n_c^{0.9} \sqrt[4]{\frac{a_1}{13d}} \text{ (dowels)} \\ n_c^{k_{ef}} \text{ (nails)} \end{cases}$		Reduction factor of the ductile capacity per shear-plane of the connection.

156 therefore propose an interaction effect for the stress components which results in a
 157 reduced capacity. They used the following interaction equation:

$$F_{i+j} = F_i \left(1 - k_{int} \frac{F_i}{F_j} \right), \text{ being } F_i \leq F_j; \quad (1)$$

158 where $k_{int} = 0.3$ is the interaction factor, and F are the plane capacities. It is considered
 159 for their model in this work.

160 3.1. Splitting failure

161 The splitting capacity of the timber members defined by the different models are
 162 given in Table 1. Splitting consists on a single crack in the vicinity of the holes (Fig-
 163 ure 3b), and it is assumed to be produced by tension perpendicular-to-the-grain. Most
 164 of the proposals contain a geometrical condition for it, with different wedge factors
 165 (relation between the perpendicular-to-grain and parallel-to-grain stresses).

166 The value of this wedge parameter, which defines the value of the perpendicular-
 167 to-grain stresses, depends on the friction between the dowel and the timber in the
 168 hole. This results in a different position (defined by an angle α) for the maximum
 169 perpendicular-to-grain stress from which the wedge value is derived. In his seminal
 170 work, Jorissen [16] considered two possibilities for this wedge parameter: $\beta_p = \frac{1}{10}$,
 171 corresponding to a friction angle $\alpha = 30^\circ$, and $\beta_p = \frac{1}{7}$ ($\alpha = 18^\circ$). As shown in Table 1,
 172 $\beta_p = \frac{1}{10}$ is used by Hanhijärvi and Kevarinmäki [22], and $\beta_p = \frac{1}{7}$ by Jockwer et al. [48],
 173 following the work of Schmid [49]. Recently, Jensen et al. [50] have found out that a
 174 higher factor $\beta_p = 0.25$ might provide a better correlation to experimental results.

175 The work from Jorissen [16], based on a Timoshenko-beam on elastic foundation
 176 accounting for the developed shear stresses by means of a Volkersen model [51], is
 177 also the basis for the effective number of fasteners n_{ef} proposed in the Eurocode 5
 178 [3], which lowers the capacity obtained by means of the EYM. This reduction factor
 179 is a way to implicitly include splitting in the design model, by reducing the ductile
 180 capacity of the connection. Since it is not properly defined as a brittle failure mode,

Table 2: Proposals for row shear failure. Shown strength refers to the capacity of the timber member, with exception of the Eurocode 5, where the reduction factor to be applied to the number of fasteners to obtain the capacity of the connection is given.

Reference	Strength	Remarks
Literature		
Hanhijärvi and Kevarinmäki [22]	$2k_{v,ctr} \frac{n_{ef}}{n_c} L_c t_{ef} f_v$	$n_{ef} = n_c^{0.9}$
Quenneville [23] [40]	$2J_r n_c n_r t a_{L,min} f_v$	$0.6 \leq J_r \leq 1$, function of n_r . $a_{L,min} = \min\{a_1, a_3\}$
Jensen and Quenneville [35]	$\min \begin{cases} 2n_c n_r t a_1 f_v \\ 2n_c n_r t a_3 f_v \\ 2\Phi t a_3 f_v^a \end{cases}$	Φ , function of fracture energy, row position (inner, outer) and connection geometry.
Standards		
Eurocode 5 [3]	$n_{ef} = \begin{cases} n_c^{0.9} \sqrt[4]{\frac{a_1}{13d}} & \text{(dowels)} \\ n_c^{k_{ef}} & \text{(nails)} \end{cases}$	Reduction factor of the ductile capacity per shear-plane of the connection.
New Zealand Standard draft [43]	$2K_{LS} 0.75 n_c n_r t a_{L,min} f_v$	$K_{LS} = \begin{cases} 0.65 & \text{(outer members)} \\ 1.0 & \text{(inner members)} \end{cases}$

Security and reduction factors from standards have been omitted

^a This expression is only valid for a symmetric connection with one fastener.

Similar expressions are derived for other configurations.

181 it is the only model which does not calculate the capacity of the timber member, but
182 obtains the splitting capacity from the ductile mode capacity per shear plane.

183 The fracture-based model developed by Jorissen [16] was later simplified by Han-
184 hijärvi and Kevarinmäki [22], and has recently been revised by Jockwer et al. [48]. In
185 terms of fracture mechanics [52], splitting can be considered a Mode I crack extension
186 (the resulting crack is produced by tension perpendicular to it) [48, 53]. The capacity
187 of fracture-based proposals is obtained from the amount of energy required to open of
188 the crack in the relevant mode, G_f . Therefore, they are very sensitive to its value (as
189 it will later be shown). In this work, the required fracture energy G_f is obtained from
190 Jockwer [48, 54].

191 3.2. Row-shear failure

192 Row-shear failure consists on two longitudinal cracks along the row of fasteners in
193 the grain direction (Figure 3c). Contrary to splitting, in terms of fracture mechanics
194 [52], it can be considered a mixed mode crack extension between Modes I and II (they
195 are produced from both tension and in-plane shear stresses) [53]. The strength of a
196 single timber member for row-shear proposed by each model is briefly described in
197 Table 2. As previously explained for splitting, no explicit model for row-shear is given
198 in the current version of the Eurocode 5 [3]. However, it is implicitly included in the
199 already referred n_{ef} [16, 51].

200 Hanhijärvi and Kevarinmäki [22] proposed a geometrical expression for the capac-
201 ity of the failure shear plane of each row. The plane is defined by the whole length
202 of the connection L_c , and a depth equal to an effective thickness, which considers the

203 influence of the dowel slenderness. Since there is an uneven load distribution among
204 the fasteners in a row, an effective number of fasteners $n_{ef} = n^{0.9}$ is used to reduce the
205 resulting capacity. Additionally, the obtained shear capacity is lowered as a result of
206 the interaction with the tension capacity in the connection, as shown in (1).

207 Another geometrical model was proposed by Quenneville [23]. However, in this
208 case, instead of the failure plane of the whole row, it is assumed that the shortest plane
209 between two fasteners (thus the one with the minimum a_1 or a_3 distances) triggers
210 the failure of the whole row. This approach was included in the Canadian Code O86
211 [39, 24], and in the New Zealand Standard draft [43] with minor differences in its
212 parameters.

213 It was found to be the plastic limit of the later developed fracture-based model
214 by Jensen and Quenneville [35, 36, 37]. For intermediate conditions, a different ex-
215 pression was proposed, in which the parameter Φ derives from a comprehensive set of
216 equations (not given in this work) which accounted for the different geometrical (spac-
217 ings –parallel and perpendicular-to-grain–, position of the row and the dowel –inner,
218 outer–...) and material properties (fracture energy) of the timber member, and the
219 chosen failure criterion (maximum shear stress or mean stress) [35–37].

220 3.3. Block-shear and plug-shear failures

221 The group-tear-out (block-shear and plug-shear, Figure 3d) failures consist on the
222 complete tear-out of the timber attached to the group of fasteners in the lateral **L**, bot-
223 tom **B** (for plug-shear) and tensile **H** planes (see Figure 4). Hence, most of the models
224 obtain the capacity of the timber member from the capacity of some or all of these
225 planes. Table 3 gives an overview of the different models, shows the capacity for each
226 failure plane (**H**, **L** and **B**), and how the capacity of the timber member is obtained as
227 a combination of those of the considered planes.

228 The models differ in the way they obtain the connection capacity from the planes’
229 capacity. Some of them propose to add the single plane capacities [55, 28], while others
230 consider as the connection capacity the minimum among the plane capacities [27, 42].

231 The proposals from the Eurocode 5 [3] and Johnsson and Parida [26] consider as
232 the joint capacity that of the plane with the maximum capacity, as the other planes
233 will have failed previously to final failure [11, 56]. Johnsson and Parida [26] take into
234 account only the bottom and head planes, because they found out experimentally that
235 the lateral planes fail in advance, and they therefore do not contribute to the ultimate
236 connection capacity.

237 Quite a different approach is given in the New Zealand draft [43] for the case of
238 plug-shear with small-diameter fasteners: based on the work by Zarnani and Quen-
239 neville [46, 29], the connection capacity is obtained from a spring model of the three
240 planes accounting for the relative stiffness Γ_i of each of them, as given in Table 5.

241 Some of the models consider an effective thickness t_{ef} for the failed planes different
242 than the whole member thickness. They are summarized in Table 4. They are mainly
243 based on the distance between the hinges in the corresponding plastic EYM mode.
244 Only the approach from Zarnani and Quenneville [46], included in the New Zealand
245 Standard draft [43], uses a beam-on-elastic-foundation model when the brittle failure
246 is produced in the elastic range, before fastener yielding, and a similar plastic-based
247 thickness for the post-elastic behaviour.

Table 3: Proposals for block-shear and plug-shear failure modes. Given capacities are those from each failure plane (**H**, **L** or **B**) of the timber member in each model.

Reference	Failure	Strength of plane			Eff. thick. t_{ef}	Remarks.
		Tensile head, H	Lateral shear, L	Bottom shear, B		
Small-diameter fasteners						
Literature						
Foschi and Longworth [27] ^a		$\frac{6b}{\sqrt{3}d} f_{t,0}$	$2 \frac{t_{ef}}{\sqrt{3}b} f_c$	\times	\times	Minimum of H or L
Kangas and Vesa [28]		$b_{net} t_{ef} f_{t,0}$	\times	$b_{net} L_{c,ef} f_c$	\checkmark	H + L
Stahl et al. [55]	L + H + B	$b_{net} f_{t,0}$	$2L_{net} f_c$	$b_c L_{c,ef} f_c$	\times	Addition, H + L + B
	H + B	$\ell (b_{net} + 2(a_4 - d)) f_{t,0}$	\times	$b L_{c,ef} f_c$	\times	Addition, H + B
	L + H	$t_{net} f_c$	$\left(\frac{6b}{2} - \ell d\right) f_{t,0}$	\times	\times	Addition, L + H
	L + H + B	$b_{net} t_{ef} f_{t,0}$	\times	$b_c L_{c,ef} f_c$	\checkmark	Maximum of H or B
Johnsson and Partida [26]		$\Gamma_B \min \left(\begin{matrix} C_{ab} 2t_{ef} L_{c,ef} f_c \\ 2t_{ef} a_4 f_{t,0} \end{matrix} \right)$	$\Gamma_B \min \left(\begin{matrix} C_{ab} 2t_{ef} L_{c,ef} f_c \\ 2t_{ef} a_4 f_{t,0} \end{matrix} \right)$	\checkmark	\checkmark	Relative stiffness of failure planes.
Zarmani and Quenneville [29, 30, 31, 46] ^b		$\Gamma_B b_c t_{ef} f_{t,0}$	$C_{ab} = k_c C_{ab}, k_e = \begin{cases} 1 & \text{if } a_4 \geq 1.25b_c \\ 0.8 & \text{if } a_4 < 1.25b_c \end{cases}$	\times	\checkmark	
Standards						
New Zealand Standard draft [43]	L + H + B	$X \Gamma_B b_c t_{ef} f_{t,0}$	$2X \Gamma_B C_b t_{ef} L_{c,ef} f_c$	\checkmark	\checkmark	Minimum of L , H or B .
	H + B	$X \Gamma_B b_c t_{ef} f_{t,0}$	\times	$X \Gamma_B C_b b L_{c,ef} f_c$	\times	Minimum of H or B .
	L + H ^c	$\Gamma_H X b_c t_{ef} f_{t,0}$	\times	$C_b = \frac{b_c}{2b_c - 1}$	\times	Minimum of H or L . k_e as in Zarmani and Quenneville [46]
Eurocode 5 [3] ^d	L + H or L + H + B	$1.5 b_{net} \ell f_{t,0}$	$0.7 f_t 2 t_{ef} L_{net}$	\checkmark	\checkmark	Maximum of H or L (+ B) Strength of B considered only for outer members not failing by embedment.
Large-diameter fasteners						
Literature						
Hanhijärvi and Kevarinmäki [22]		$k_{c,anar} \frac{b_{net}}{b_c} (a_2 - d) f_{t,0}$	$2k_{c,anar} \frac{b_{net}}{b_c} [(n_c - 1) a_1 + a_3] t_{ef} f_c$	\times	\checkmark	Interaction of shear and tension, Addition of inner and outer parts. $1.7 \leq k_{c,anar} \leq 2$; $0.7 \leq k_{c,anar} \leq 1$ $a_{L,min} = \min(a_1, a_3)$
Quenneville [23] [40]	L + H	$t (n_c - 1) (a_2 - (d + 2)) f_{t,0}$	$2n_c n_c t f_c a_{L,min}$	\times	\times	
New Zealand Standard draft [43]	L + H	$1.25 b_{net} t f_{t,0}$	$2K_{LS} 0.75 n_c t a_{L,min} f_c$	\times	\times	
Eurocode 5 [3] ^d	L + H or L + H + B	$1.5 b_{net} \ell f_{t,0}$	$0.7 f_t 2 t_{ef} L_{net}$	\checkmark	\checkmark	Maximum of H or L (+ B) Strength of B considered only for outer members not failing by embedment.

\times implies the plane or concept is not addressed in the model

\checkmark implies t_{ef} is considered and defined in Table 4

Security and reduction factors from standards have been omitted

^a K_t , β_t , α_t , and γ_t are coefficients based on geometric parameters.

^b When only the failure of two planes is considered, the capacity of the third is dismissed.

Γ denotes additional expressions related to the relative stiffness of each failure plane. See Table 5

^c t is taken when only one side of the member is loaded; otherwise, $\frac{t}{2}$

^d Chosen according to the yield mode. Second line for embedment modes.

Table 4: Effective thickness considered on the different approaches for block-shear and plug-shear failures in Table 3.

Reference	Domain	Expression	Remarks
Small-diameter fasteners			
Kangas and Vesa [28]		$2\sqrt{\frac{M_y}{f_{h,0}d}}$	
Johnsson and Parida [26]		$2\sqrt{\frac{M_y}{f_{h,0}d}}$	
Zarnani and Quenneville [29, 30, 31, 46]	Elastic	$\begin{cases} 0.95\ell & \text{when } \ell = 28.5\text{mm} \\ 0.85\ell & \text{when } \ell = 53.5\text{mm} \\ 0.75\ell & \text{when } \ell = 78.5\text{mm} \end{cases}$	Beam on elastic foundation model. Linear interpolation for intermediate values of ℓ .
	Mixed mode	$\begin{cases} \ell & \text{(embedding)} \\ \sqrt{\frac{M_{c,y}}{f_{h,0}d_r} + \frac{\ell^2}{2}} & \text{(one hinge)} \\ 2\sqrt{\frac{M_{c,y}}{f_{h,0}d_r}} & \text{(two hinges)} \end{cases}$	
Standards			
New Zealand draft [43]	Elastic	$C_0 J_y t$ $J_y = \begin{cases} 1.0 & \text{if } t_p \geq 6.3\text{mm} \\ 0.9 & \text{if } 4.7\text{mm} \leq t_p \leq 6.3\text{mm} \\ 0.8 & \text{if } 3.2\text{mm} \leq t_p \leq 4.7\text{mm} \end{cases}$ $C_0 = \begin{cases} 0.95 & \text{if } \ell = 28.5\text{mm} \\ 0.75 & \text{if } \ell = 78.5\text{mm} \end{cases}$	Linear interpolation for intermediate values of ℓ .
	Post-yield	$\begin{cases} J_y \sqrt{\frac{M_{c,y}}{d_r f_{r,0}} + \frac{\ell^2}{2}} & \text{(one hinge)} \\ 2J_y \sqrt{\frac{M_{c,y}}{d_r f_{r,0}}} & \text{(two hinges)} \end{cases}$	
Eurocode 5 [3]	Thin plates	$\begin{cases} 0.4\ell & \text{(no hinges)} \\ 1.4\sqrt{\frac{M_y}{f_{h,0}d}} & \text{(one hinge)} \\ 2\sqrt{\frac{M_y}{f_{h,0}d}} & \text{(two hinges)} \end{cases}$	
	Thick plates	$\ell \left[\sqrt{2 + \frac{M_y}{f_{h,0}d\ell^2}} - 1 \right] \text{ (one hinge)}$	
Large-diameter fasteners			
Hanhijärvi and Kevarinmäki [22]		$\begin{cases} \min \left\{ \begin{array}{l} t \\ 1.47\sqrt{\frac{1.5f_{h,0}}{f_y}} \end{array} \right. & \text{(side members)} \\ \min \left\{ \begin{array}{l} t \\ 0.615\sqrt{\frac{1.5f_{h,0}}{f_y}} \end{array} \right. & \text{(middle members)} \end{cases}$	Characteristic value for $f_{h,0}$; mean value for f_y .
Standards			
Eurocode 5 [3]	Thin plates	$\begin{cases} 0.4t & \text{(no hinges)} \\ 1.4\sqrt{\frac{M_y}{f_{h,0}d}} & \text{(one hinge)} \\ 2\sqrt{\frac{M_y}{f_{h,0}d}} & \text{(two hinges)} \end{cases}$	
	Thick plates	$t \left[\sqrt{2 + \frac{M_y}{f_{h,0}d\ell^2}} - 1 \right] \text{ (one hinge)}$	

Security and reduction factors from standards have been omitted
 d_r , $f_{r,h,0}$ and $M_{c,y}$ are the diameter, embedment strength and yielding moment capacity for rivets.
Rivets have a rectangular cross-sectional area of 6.4 mm by 3.2 mm. $d_r = 3.2\text{mm}$.

Table 5: Stiffness parameters for the *New Zealand* approach for plug-shear failure.

Reference	Γ_H	Γ_B	Γ_L
Zarnani and Quenneville [31] ^{a,b}	$\frac{K_H+K_B+K_L}{K_H}$	$\frac{K_H+K_B+K_L}{K_B}$	$\frac{K_H+K_B+K_L}{K_L}$
Used parameters	$K_H = \frac{2Eb_c t_{ef}}{L_c - a_3}$	$K_B = (1 - H)(K_{sb} + K_{tb})$ $K_{sb} = \frac{GL_c b_c}{2t_{ef}}$ $K_{tb} = \frac{Eb_c t_{ef}}{5(L_c - a_3)}$ $H = \begin{cases} 0 & \text{if } (t - t_{ef}) \geq 2t_{ef} \\ 0.25 \left(3 - \frac{t}{t_{ef}}\right)^2 & \text{if } (t - t_{ef}) < 2t_{ef} \end{cases}$	$K_L = (1 - F)(K_{sl} + K_H)$ $K_{sl} = \frac{2L_c t_{ef} G}{b_c}$ $K_H = \frac{Eb_c t_{ef}}{5(L_c - a_3)}$ $F = \begin{cases} 0 & \text{if } a_4 \geq 1.25b_c \\ 0.16 \left(2.5 - \frac{2a_4}{b_c}\right)^2 & \text{if } a_4 < 1.25b_c \end{cases}$
Standards			
New Zealand Standard draft [43] ^c	$1 + \lambda_1 + \lambda_2$	$1 + \frac{1}{\lambda_1} + \lambda_3$	$1 + \frac{1}{\lambda_2} + \frac{1}{\lambda_3}$
	$\lambda_1 = \frac{K_B}{K_H}$	$\lambda_2 = \frac{K_L}{K_H}$	$\lambda_3 = \frac{K_L}{K_B}$

^a Equations are rewritten according to the nomenclature used in this paper.

^b When only two planes are involved, the stiffness of the third is dismissed.

^c Defines λ_i parameters for ease of use. Their relationship to [31] is given.

Table 6: Tests on connections with large-diameter fasteners loaded parallel-to-the-grain. Some tests reported more than one failure mode, so the sum of percentages is higher than 100%.

	Jensen and Quenneville [37]	Mohammad and Quenneville [40]	Quenneville and Mohammad [39]	Sjödin and Johansson [47]	Iraola [57]	Hanhijärvi and Kevarinmäki [22]	Total
No. of config.	16	30	46	6	13	30	141
No. of tests	104	300	460	30	38	98	1030
Joint scheme (Figure 2)							
WS (Fig.2c)	–	9	–	–	–	–	9
SWS (Fig.2d)	16	–	46	–	–	17	63
WSW (Fig.2e)	–	21	–	6	13	13	53
Joint config.							
1 fastener	8	9	6	–	3	–	26
1 row	8	8	1	–	10	–	27
Group	–	13	39	6	–	30	88
Fastener							
Bolt	16	30	46	–	–	–	92
Dowel	–	–	–	6	13	30	49
Timber product							
LVL	16	–	–	–	–	17	33
GL	–	22	45	6	–	13	86
Lumber	–	8	1	–	13	–	22
Failure mode							
Ductile	3	–	9	–	–	–	12
Splitting	14	1	9	–	13	–	37
Row	–	22	26	6	–	3	57
Block	–	18	11	3	–	26	58
Tension	–	–	–	–	–	3	3

248 4. Procedure for the benchmarking of design approaches by experiments

249 4.1. Experimental data reported in literature

250 A summary of tests related to brittle failure on connections loaded parallel-to-grain
251 reported in literature is given in Table 6 for large diameter fasteners (bolts and dow-
252 els) and Table 7 for small-diameter fasteners (nails and rivets). Both provide a brief
253 description of the main features of the compiled data set, such as number and type
254 of configurations tested (as described in Figure 2), used timber product, and reported
255 failure mode. All the compiled tests are tension tests.

256 Some works analyzed the influence of the moisture content and its variation in the
257 brittle capacity (i.e. Sjödin and Johansson [47]). Only those tests where the timber
258 members were around the reference moisture content of 12% were considered.

259 In the case of large-diameter fasteners, more than a thousand individual tests, grouped
260 in 141 different configurations conform the database. Almost all of them are double-
261 shear configurations, with a central steel plate (WSW, 42.4%) or with side steel plates
262 (SWS, 50.4%). Some of the featured tests are single dowel (18.4%) and single-row

Table 7: Tests on connections with small-diameter fasteners loaded parallel-to-the-grain.

		Zarnani and Quenneville [46]	Zarnani and Quenneville [29]	Foschi and Longworth [27]	Johnsson and Parida [26]	Total	
No. of config.		32	8	10	22	72	–
No. of tests		102	24	30	91	247	–
Joint scheme (Figure 2)	WS (Fig.2a)	–	–	10	22	32	44.4%
	SWS (Fig.2b)	32	8	–	–	40	55.6%
Fastener	Rivet	32	8	19	–	50	69.4%
	Nail	–	–	–	22	22	30.6%
Timber product	LVL	6	8	–	–	14	17.9%
	GL	26	–	10	22	64	82.1%
Failure mode	Ductile	4	2	2	1	9	11.5%
	Brittle	28	6	8	21	69	88.5%

263 (19.2%) connections, which may not reflect practice. However, 62.4% of the connec-
 264 tions are group of fasteners, more similar to current practice. Different types of timber
 265 products are present, being glulam (61%) the best represented. From the perspective
 266 of the different failure modes, the majority of them failed in a brittle mode. Around
 267 40% of the brittle failures are row-shear or block-shear. Only 26% failed due to split-
 268 ting. However, this type of failure is mostly seen in connections with a single row or
 269 fastener, which are not common in practice.

270 A total of 72 different connection configurations (247 individual tests), with roughly
 271 half of them in a WS single-shear configuration and the other half in double-shear SWS
 272 have been compiled for small-diameter fasteners. From them, 88.5% experienced brit-
 273 tle failure. Most of the tests used rivets (69.4%) as fasteners.

274 It is worth noticing that some of the tests come from the experimental campaign
 275 originally developed to derive some of the models. In those cases, they conform the
 276 validation space against which those particular models were originally calibrated.

277 4.2. Benchmarking procedure

278 4.2.1. Levels of comparison

279 Two different levels of comparison may be established for the comparison of the
 280 models and the experimental results: mean and characteristic. However, literature usu-
 281 ally reports experimental mean values and the corresponding coefficient of variation,
 282 while the different material properties are usually given at the characteristic level.

283 Since most of the compiled tests have few replicates, (usually three, and just a
 284 few of them as much as ten [40]), obtaining a relevant characteristic test value [58] as
 285 desirable, is nevertheless doubtful.

286 To provide a common framework and methodology, the corresponding material
 287 properties used in the model for each test are taken from the relevant standards or other
 288 available technical documentation [59, 60, 38, 32, 61] according to the type of product
 289 and originally reported strength class (all the compiled tests provided such informa-
 290 tion). However, as said, the given strength values are at a characteristic level and must
 291 be converted to mean values to allow the comparison to the mean experimental values.
 292 The probabilistic model for timber proposed by the JCSS [62] has been used to obtain
 293 the required mean material properties with a script developed within the framework of
 294 the COST Action FP1402 [63, 64].

295 The same procedure was done to obtain the mean fastener properties from the nom-
 296 inal properties, by means of the corresponding probabilistic model [65]. However, the
 297 influence of the steel properties is quite irrelevant, with the exception of the n_{ef} param-
 298 eter in the Eurocode 5.

299 Therefore, both test results and material properties are assessed at the mean level.
 300 However, although not discussed here, the comparison at the characteristic level was
 301 done as well, providing similar results.

302 4.2.2. Metrics to measure model performance

303 It is advisable to use more than one metric to provide an adequate evaluation of the
 304 performance of the different models [66–71]. It is suggested to calculate them at a 95%
 305 confidence level, after eliminating the tests with the highest residuals to dismiss any
 306 outlier predictions, judging or measurement errors [70]. The sections below provide an
 307 explanation of the different metrics used for the performance assessment in this work.

308 No single metric can replace a scatter plot in which the experimental results are
 309 compared to the model results. A complementary visual inspection of the scatter plots
 310 is always needed in order to notice problems which the metrics may obscure [72].
 311 Hence, the corresponding scatter plots are given as a reliable tool to additionally esti-
 312 mate the calibration of each model in Figures 5 to 8.

313 *Overall performance measures.*

314 **Coefficient of determination** A general procedure to verify model fitting of the
 315 models is the coefficient of determination Q^2 [66, 73],

$$Q^2 = 1 - \frac{\sum_{i=1}^n (y_i - f_i)^2}{\sum_{i=1}^n (y_i - \bar{y})^2}, \quad (2)$$

316 where y_i are the observed experimental values, f_i are the predicted values by the mod-
 317 els, and \bar{y} is the mean of the experimental values. Eq. (2) may give negative values
 318 [68] when it is not applied to regression fitting, as is the case herein. In those cases (as
 319 it will be shown) it is just a proof of poor prediction ability. A reliable threshold value
 320 for Q^2 has been found to be 0.70 [72]. Although extensively used, the validity of the
 321 Q^2 metric as a reliable source to assess performance of models is highly questionable
 322 [67–70].

323 Additional criteria and different metrics to verify the validity of a model have been
 324 proposed as replacement [67, 68]. In this study, the concordance correlation coefficient
 325 (CCC) [71, 73, 72] is used. It is here rewritten for the current comparison case as

$$CCC = \frac{2 \sum_{i=1}^n (f_i - \bar{f})(y_i - \bar{y})}{\sum_{i=1}^n (f_i - \bar{f})^2 + \sum_{i=1}^n (y_i - \bar{y})^2 + n(\bar{f} - \bar{y})^2}, \quad (3)$$

326 where n is the number of experiments, and \bar{f} the mean of the predicted values. This pa-
 327 rameter measures both precision (error between the predictions f_i and the experimental
 328 values y_i) and accuracy (how much the model deviates from the slope 1 line passing
 329 through the origin). It has been demonstrated to be more reliable than other similar
 330 metrics for model validation, with a recommended threshold value of 0.85 [73, 72].

331 **Error measurement** In order to obtain a simple expression of the error, the mean
332 relative error *MRE* is defined as

$$MRE = \frac{1}{n} \frac{\sum_{i=1}^n |y_i - f_i|}{\bar{y}}. \quad (4)$$

333 Relative errors of around 10% are usually agreed as adequate. The standard deviation
334 of this mean error *SD* will be given as well.

335 **Correlation** Additionally, it can be of interest to find models which are able to
336 provide a good correlation, although they may provide quantitatively wrong predic-
337 tions. Two different correlation measurements are used in this work.

338 A rank correlation coefficient *c* [68] provides information on the relative ranking,
339 that is, on the ability of each model to order the tests correctly according to their ca-
340 pacity, independently of the quantitative predictions. A higher correlation coefficient
341 implies a better model.

342 The slope *m* of a linear fit passing through the origin is another way to measure
343 the observed correlation between values. Although it provides no adequate measure of
344 the degree of accuracy [68], it gives an idea of how conservative or unconservative the
345 model is. Slopes close to one are usually proof of a good model correlation.

346 *Evaluation of characteristic over-prediction, R_5 .* The final aim of this review is to con-
347 sider the models as candidates for a future design standard. Such documents are written
348 to provide predictions at a characteristic level, which is further transformed to a design
349 level. A good model, previously to the use of additional factors in the code, should pro-
350 vide a performance similar to a 5-percentile (*characteristic*) prediction, meaning that
351 the capacity of a number of tests close to the 5-percentile of the total number should be
352 over-predicted, and the capacity of most of the tests should be under-predicted.

353 Therefore, as an additional check, the corresponding metric R_5 is evaluated. It
354 represents the relative amount of tests for which the models, when they are used with
355 characteristic material properties, over-predict the mean test value. A value for this
356 parameter of 0.05 (5%) or lower, would mean a better fit of the model within the current
357 design standards practice, as it fulfills the safety condition that approximately only 5%
358 of the tests are over predicted.

359 *Discrimination.* The validity of a model can be related as well to its ability to discrim-
360 inate between brittle and ductile failures [66]. Therefore, such discrimination power is
361 also assessed in this work (see Section 5.5).

362 5. Results of the benchmarking

363 For the assessment of the reviewed proposals, each approach is evaluated against
364 those tests which have been reported to fail in such manner, i.e. the splitting methods
365 are evaluated against the connections which have been reported to fail in splitting.

Table 8: Splitting. Comparison of the different models, ordered from the highest (best) to the lowest CCC .

Model	Q^2	$MRE (SD)$	m	c	CCC	R_5
Eurocode 5 [3]	0.736	0.263 (0.304)	1.057	0.872	0.868	0.444
Jockwer et al. [48]	0.422	0.338 (0.368)	0.970	0.705	0.719	0.037
Hanhijärvi and Kevarinmäki [22]	-2.498	0.786 (0.948)	1.616	0.794	0.487	0.444
Jorissen [16]	-0.162	0.518 (0.483)	0.474	0.615	0.342	0.074

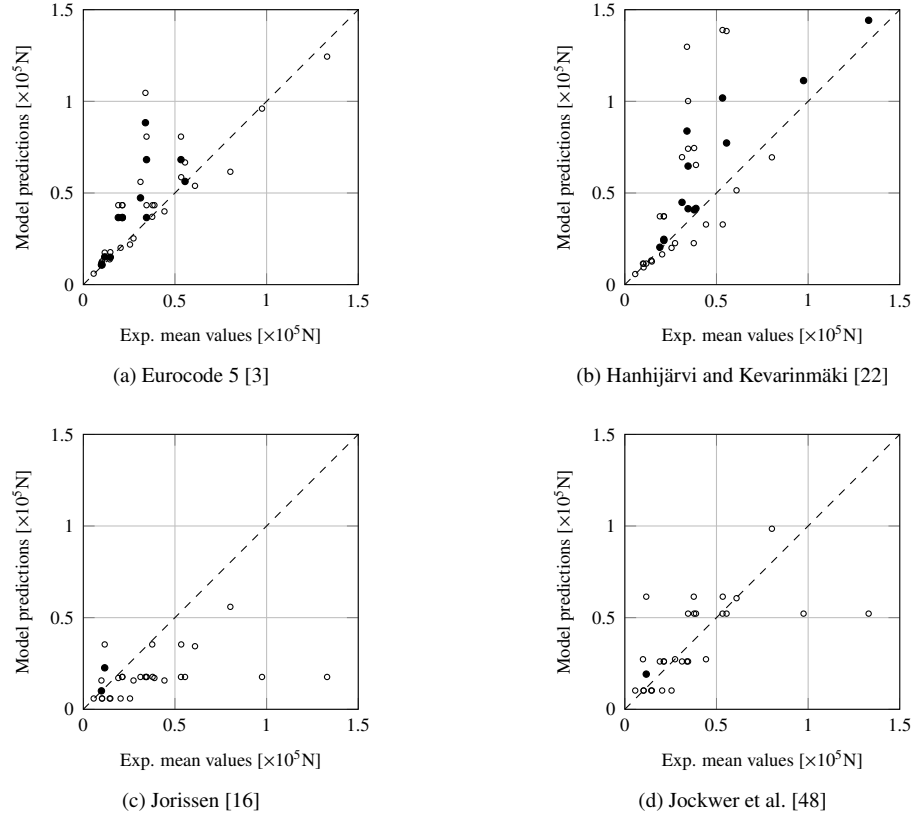


Figure 5: Splitting. Scatter plots of the experimental mean results and the predicted value from different approaches (with mean material properties). Filled dots represent the values that are overpredicted when characteristic material properties are applied, represented by R_5 .

366 *5.1. Splitting*

367 The results for the benchmarking of the different splitting models are given in Ta-
368 ble 8, with the corresponding scatter plots in Figure 5.

369 Just two of the models, Eurocode 5 [3] and Jockwer et al. [48] have a positive
370 coefficient of determination Q^2 . On the other hand, Hanhijärvi and Kevarinmäki [22]
371 and Jorissen [16] obtain a negative Q^2 . This lack of predictive ability is additionally
372 proved by their mean error, which is higher than 0.5. It is clear in the corresponding
373 scatter plots, Figs. 5b and 5c.

374 The slopes of the fitted linear regression through the origin m are an additional
375 proof of the predicting ability of the different models. Those models with a positive
376 coefficient of determination have a slope close to one, while the others do not obtain
377 such a good agreement: Hanhijärvi and Kevarinmäki [22] tends to overpredict, and
378 Jorissen [16] to underpredict.

379 The correlation coefficient c provides a different point of view, as it does not con-
380 sider the quantitative agreement. The best correlated model, Eurocode 5 [3], is the one
381 with the highest Q^2 coefficient; but the second best, Hanhijärvi and Kevarinmäki [22],
382 is the one with the worst Q^2 . However, only the ability of the model to order the results
383 in the correct order is assessed which, for cases such as the one studied here, may not
384 be not enough.

385 It is interesting to notice how the CCC parameter provides an appropriate summary
386 of the precedent metrics. The Eurocode model [3] gets a score over the defined thresh-
387 old for a good model ($CCC \geq 0.85$). Jockwer et al. [48] gets the second best CCC
388 coefficient, and due to its better correlation performance, the model of Hanhijärvi and
389 Kevarinmäki [22] get the third best value, although it obtained a negative Q^2 .

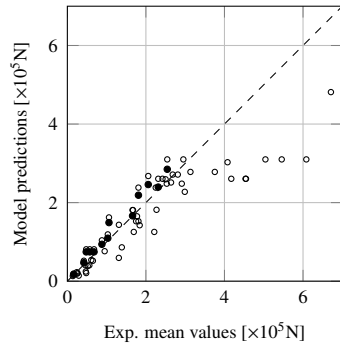
390 The fracture-based model from Jorissen [16] obtains the worst result. However,
391 one important remark must be made: due to the lack of availability of the fracture
392 energy values for the different timber products, the same value for lumber (obtained
393 from Jockwer [54]) had to be used for the whole data set. Fracture energy values are
394 yet to be included in daily available technical documents in order for these models to
395 be used.

396 Only the models from Jockwer et al. [48] and Jorissen [16] obtain low R_5 values,
397 close to the desired threshold of 0.05. However, this fact could be improved for the
398 other models by means of a calibration parameter. The over-predicted tests are filled in
399 black in Figure 5, to provide a feeling about their number and distribution.

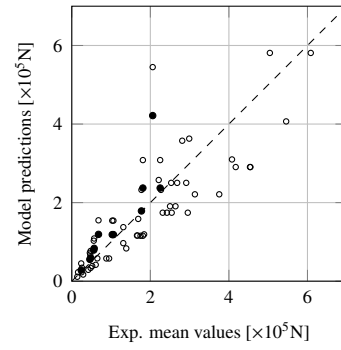
400 *5.2. Row-shear failure*

401 In the previous section, it was shown how the CCC metric provides a simple way
402 to measure the performance of the models, in a similar way to what it is reflected in
403 the corresponding scatter plots and in the different additional metrics. For the sake
404 of brevity, the following discussion will mainly refer to this CCC parameter. The
405 corresponding Tables will still show the remaining metrics for completeness.

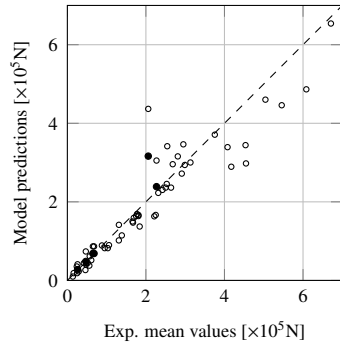
406 When looking at the plots of the different models in Figure 6, two of the models,
407 New Zealand Standard draft [43] and Hanhijärvi and Kevarinmäki [22], obtain values
408 close to the ideal correlation depicted with the dashed line. Due to its lower scatter
409 and error, the model from Hanhijärvi and Kevarinmäki [22] gets the best CCC value.



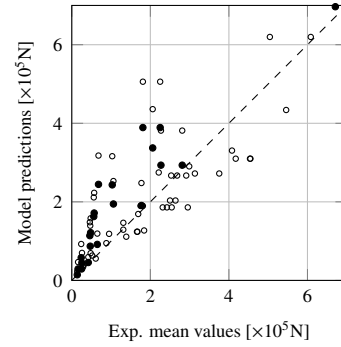
(a) Eurocode 5 [3]



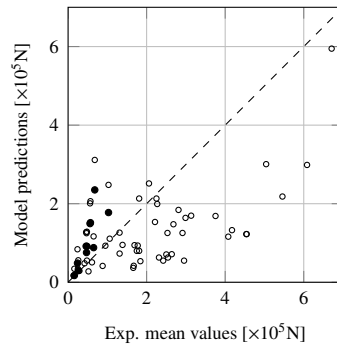
(b) New Zealand Standard draft [43]



(c) Hanhijärvi and Kevarinmäki [22]



(d) Quenneville [23]



(e) Jensen and Quenneville [35]

Figure 6: Row-shear failure. Scatter plots of the experimental mean results and the predicted value from different approaches (with mean material properties). Filled dots represent the values that are overpredicted when characteristic material properties are applied (R_5).

Table 9: Row-shear failure. Comparison of the different models, ordered from the highest to the lowest CCC .

Model	Q^2	$MRE (SD)$	m	c	CCC	R_5
Hanhijärvi and Kevarinmäki [22]	0.928	0.142 (0.159)	0.910	0.977	0.961	0.105
New Zealand Standard draft [43]	0.780	0.279 (0.224)	0.855	0.913	0.877	0.228
Eurocode 5 [3]	0.778	0.227 (0.278)	0.803	0.942	0.862	0.228
Quenneville [74]	0.635	0.353 (0.328)	1.003	0.794	0.819	0.386
Jensen and Quenneville [35]	0.182	0.556 (0.455)	0.560	0.483	0.486	0.193

Table 10: Block shear failure. Comparison of the different models, ordered from the highest to the lowest CCC .

Model	Q^2	$MRE (SD)$	m	c	CCC	R_5
Hanhijärvi and Kevarinmäki [22]	0.552	0.180 (0.182)	1.134	0.939	0.826	0.227
New Zealand Standard draft [43]	-0.045	0.290 (0.234)	0.898	0.688	0.569	0.159
Quenneville [74]	-0.483	0.277 (0.348)	1.196	0.711	0.528	0.273
Eurocode 5 [3]	-0.286	0.319 (0.263)	0.919	0.613	0.523	0.159

410 It also obtains the lowest (and therefore best) R_5 metric, with a 10% of the tests over
 411 predicted for characteristic values in the model.

412 The implicit model of the Eurocode 5 [3], the n_{ef} parameter, gets a good CCC
 413 metric, slightly worse than that of the New Zealand Standard draft [43]. The scatter
 414 plot (Fig. 6a) shows a reduction on its prediction ability for high capacities, which it
 415 tends to under-predict. It may be related to the fact that it is a reduction factor of the
 416 EYM ductile capacity. The higher error in the high-capacity region of the Eurocode 5
 417 [3] model is described by the standard deviation metric of the model, shown in brackets
 418 in Tab. 9, higher than the one of the New Zealand Standard draft [43].

419 As happened in the previous Section for the fracture-based splitting model of Jorisen
 420 [16], the fracture-based model from Jensen and Quenneville [37] gets the worst
 421 score. However, as noted above, it is not a proof of worse predicting ability, but of the
 422 lack of information available on the fracture energy G_f .

423 5.3. Block-shear failure

424 The results for the benchmarking of the different block models are given in Ta-
 425 ble 10. Only the model from Hanhijärvi and Kevarinmäki [22] gets a good value of the
 426 CCC metric, with comparable performance in the other metrics.

427 Due to the huge variety of different configurations in the experimental tests and the
 428 high range of analysed data, all the remaining models obtain negative coefficients of
 429 determination Q^2 . However, the scatter plots do not describe such a bad agreement, as
 430 also proved by their correlation factors ($c \geq 0.6$), and their CCC values, around 0.5 for
 431 all of them. The negative Q^2 values are mainly due to the fact of the high mean errors
 432 and corresponding standard deviations obtained.

433 5.4. Plug-shear failure

434 The results for the benchmarking of the different plug-shear models are given in
 435 Table 11. Additionally, since the models were originally proposed for different fasten-

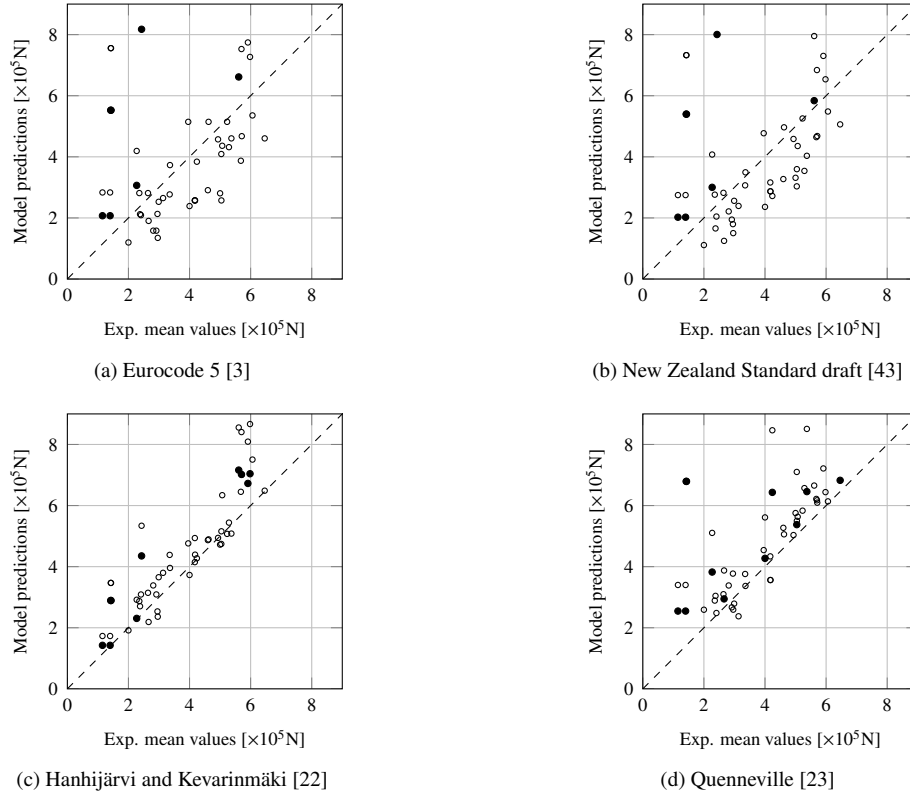
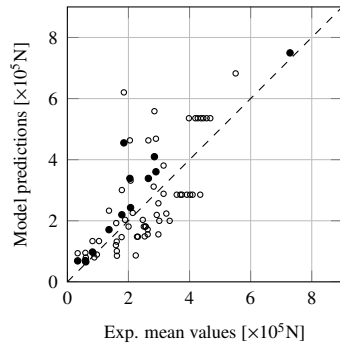


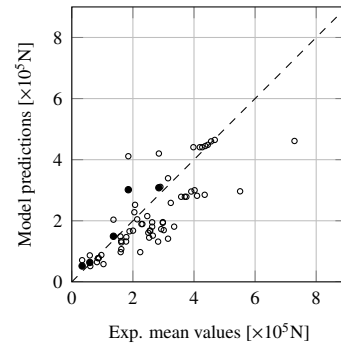
Figure 7: Block-shear failure. Scatter plots of the experimental mean results and the predicted value from different approaches (with mean material properties). Filled dots represent the tests that are overpredicted when characteristic material properties are applied (R_5).

Table 11: Plug-shear failure. Comparison of the different models, ordered from the highest to the lowest CCC.

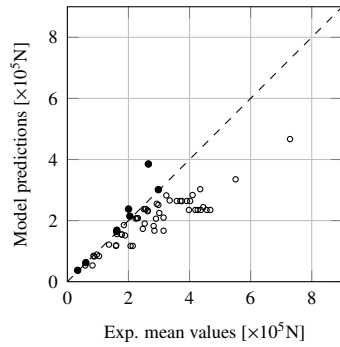
Model	Q^2	$MRE (SD)$	m	c	CCC	R_5
Kangas and Vesa [28]	0.700	0.224 (0.144)	0.983	0.895	0.874	0.150
New Zealand Standard draft [43]	0.535	0.239 (0.182)	0.831	0.846	0.788	0.083
Eurocode 5 [3]	0.359	0.310 (0.193)	0.979	0.787	0.754	0.217
Johnsson and Parida [26]	0.385	0.257 (0.241)	0.730	0.839	0.638	0.133
Stahl et al. [55]	-4.780	0.977 (0.69)	1.955	0.891	0.403	0.833



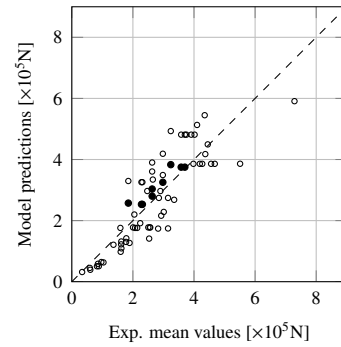
(a) Eurocode 5 [3]



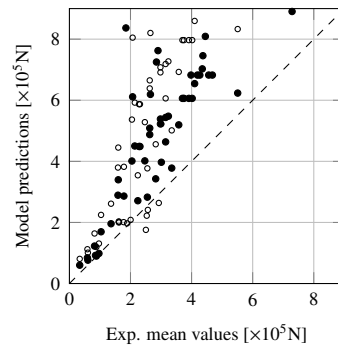
(b) New Zealand Standard draft [43]



(c) Johnson and Parida [26]



(d) Kangas and Vesa [28]



(e) Stahl et al. [55]

Figure 8: Plug-shear failure. Scatter plots of the experimental mean results and the predicted value from different approaches. Filled dots represent the values that are overpredicted when characteristic material properties are applied (R_5).

Table 12: Plug-shear failure. Influence of the different type of fastener (nails or rivets) in the performance of the models.

Model	Nails			Rivets		
	Q^2	$MRE (SD)$	CCC	Q^2	$MRE (SD)$	CCC
Kangas and Vesa [28]	0.502	0.301 (0.185)	0.712	0.669	0.228 (0.168)	0.826
New Zealand Standard draft [43]	0.404	0.315 (0.225)	0.582	0.218	0.231 (0.2)	0.687
Eurocode 5 [3]	0.409	0.322 (0.212)	0.591	0.413	0.318 (0.188)	0.783
Johnsson and Parida [26]	0.830	0.135 (0.159)	0.903	-0.191	0.307 (0.218)	0.436
Stahl et al. [55]	0.350	0.317 (0.252)	0.669	-6.016	1.181 (0.485)	0.284

436 ers, namely nails and rivets, Table 12 shows a summary of the obtained values for the
 437 tests with each type of connector (nails or rivets).

438 Most of the available tests have been made for rivets (only the tests from Johnsson
 439 and Parida [26] were done with nails –see Table 7–) and, therefore, most of the propos-
 440 als have been validated for rivets, not for nails. The only ones which were developed
 441 for nails are those from Eurocode 5 [3] and Johnsson and Parida [26]. However, and
 442 since brittle failure is related to timber, it may be assumed that, for similar connection
 443 areas, the type of connector might play a minor role in the resulting brittle capacity.

444 The model from Kangas and Vesa [28] qualifies as the best predictor, as proved by
 445 its superior metrics.

446 The model in the New Zealand Standard draft [43] gets the second position in terms
 447 of the concordance correlation coefficient. It gets a lower coefficient of determination,
 448 comparable error and tends to underpredict, as shown by its slope. However, maybe
 449 due to this fact it gets the best ratio for characteristic values in the model. The model
 450 in the Eurocode 5 [3] gets a similar CCC value, thanks to its good slope, although the
 451 remaining metrics are worse, including the performance at characteristic level.

452 The model from Stahl et al. [55] consistently over-predicts, as shown in Fig. 8e, and
 453 therefore gets the worst CCC value. However, it obtains one of the highest correlation
 454 factors. It is the only studied model which does not use an effective thickness t_{ef} .

455 Due to the fact that two quite different small-diameter fasteners are used in the
 456 experimental data set (round nails, and rectangular rivets), it is interesting having a
 457 look at the performance of the different models for each fastener type, as shown in
 458 Table 12. The model proposed by Johnsson and Parida [26] surpasses the others in the
 459 case of nails. However, being theirs the only tests with nails, it is just a proof of the
 460 good validation with their own tests. Kangas and Vesa [28] obtains the second best
 461 CCC score. The model from Johnsson and Parida [26] gets lower performance when
 462 compared only to those tests with rivets, while the remaining models (proposed for
 463 rivets) improve. The model from Kangas and Vesa [28] remains as one of the best.

464 5.5. Discrimination ability

465 As previously explained, an additional interesting metric in this particular study
 466 is the ability to correctly predict the failure mode of the connection, whether ductile
 467 or brittle. An additional consideration would be related to the safety level for false
 468 predictions: predicting a false ductile failure could lead to unsafe results; while a false
 469 brittle prediction would lead to a conservative design.

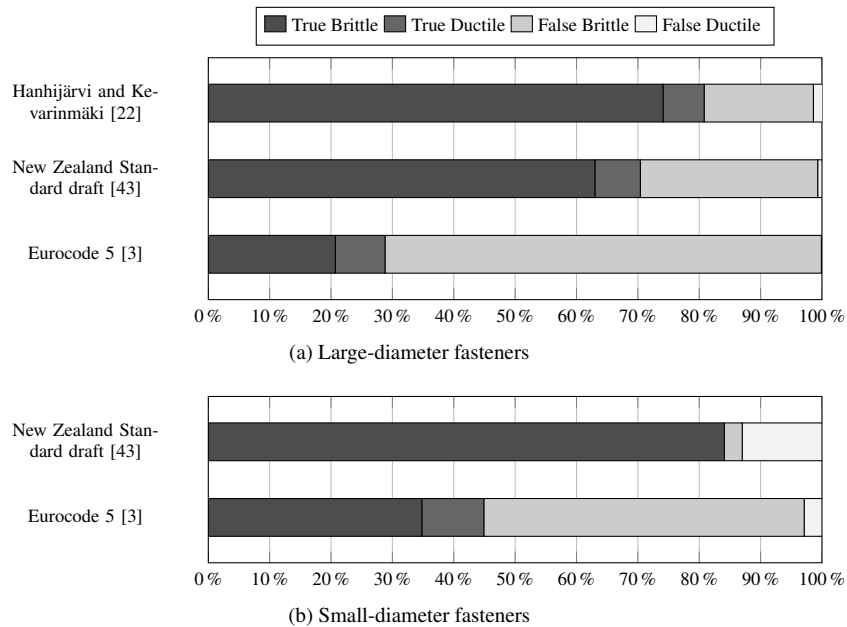


Figure 9: Discrimination ability. Comparison between Eurocode 5 [3], New Zealand Standard draft [43] and Hanhijärvi and Kevarinmäki [22].

470 Only the design standards, Eurocode 5 [3], New Zealand Standard draft [43], and
 471 the proposal from Hanhijärvi and Kevarinmäki [22] are somehow comprehensive pro-
 472 posals which allow for a complete discrimination for dowels; and only the design stan-
 473 dards [3, 43] allow for it in the case of small-diameter fasteners. The rest of the re-
 474 viewed models are models for a single failure mode.

475 However, the system proposed in the current Eurocode faces a problem when eval-
 476 uated this way. Since it does not explicitly consider splitting or row-shear, it cannot
 477 predict a ductile failure: the supposed *ductile* EYM failure is always a brittle failure,
 478 as it is always the result of reducing the ductile capacity with the n_{ef} parameter. Only
 479 those tests with a single fastener (not allowed in the Eurocode, but in which the n_{ef} is
 480 not applied) can be classified as ductile failure.

481 In the case of large-diameter fasteners (dowels and bolts), the model from Hanhi-
 482 järvi and Kevarinmäki [22] provides the best discrimination ability, as shown in Fig-
 483 ure 9a. It correctly predicts over 80% of the failure modes (either ductile or brittle).
 484 Not surprisingly, it is consistently ranked as one of the best models for each single
 485 failure mode. The model in the New Zealand Standard draft [43] gets a slightly lower
 486 discrimination ability (70.4%), much higher than that obtained with the Eurocode 5 [3]
 487 (28.9%).

488 For small-diameter fasteners (Figure 9b), the New Zealand Standard draft [43] is
 489 clearly superior to the Eurocode 5 [3]. It correctly predicts over 85.5% of the compiled
 490 experimental sets, against less than 44.9% for the Eurocode 5 [3].

491 6. Conclusions

492 Having reliable models to verify the brittle failure of timber connections is of ut-
493 most importance. This paper reviews several existing models (explained in Sect. 3)
494 for brittle failure of timber connections loaded in the parallel-to-grain direction. Their
495 performance against a set of tension tests gathered from literature (Tables 6 and 7) has
496 been compared. The compared models allow to evaluate splitting (Tab. 1), row-shear
497 (Tab. 2), and block and plug-shear (Tab. 3) failures. Special attention has been given to
498 the models included in two design standards, current Eurocode 5 [3] and New Zealand
499 Standard draft [43].

500 The comparison has been made at the mean level, and for that, the characteristic
501 material properties have been converted to mean values by means of a probabilistic
502 model [62].

503 The use of the metric CCC (3) has been proposed. It provides a useful measure
504 of the validity of the models, and it has been shown to give a summary of the other
505 metrics (coefficient of determination, mean error, correlation and fitting slope). In any
506 case, it does not replace the scatter plots of experimental and predicted values, which
507 give a clear view of the models' validity.

508 The n_{ef} model included in the current Eurocode 5 [3] for splitting and row-shear is
509 the best for splitting. However, this implicit inclusion of failure modes is not advisable,
510 since it does not inform in an appropriate way to the designer about the expected failure
511 mode. The models from Hanhijärvi and Kevarinmäki [22] and New Zealand Standard
512 draft [43] get better results in the case of row-shear.

513 The Annex A of Eurocode 5 [3], which deals with block and plug-shear is one of
514 the least reliable models. It is the worst model for block-shear, where the model from
515 Hanhijärvi and Kevarinmäki [22] is the best one; and it is surpassed by the models from
516 Kangas and Vesa [28] and New Zealand Standard draft [43] for plug-shear failure.

517 The model for dowelled connections developed by Hanhijärvi and Kevarinmäki
518 [22] gets the best results for row-shear and block-shear failures. At the same time, it is
519 the model which best discriminates ductile and brittle failure for large-diameter fasten-
520 ers. It seems as a viable alternative to the models currently included in the standards
521 for dowelled connections.

522 The New Zealand Standard draft [43] consistently gets the second best position in
523 its considered failure modes: row-shear, block-shear and plug-shear. It does not take
524 splitting into account which is, however, a rare failure in current practice connections
525 with more than one row. At the same time, it gets the best discrimination ability as a
526 comprehensive system for both large and small-diameter fasteners.

527 In the case of plug-shear, a simple model such as the one proposed by Kangas
528 and Vesa [28] is the best one, instead of more elaborate alternatives, such as the one
529 developed by Zarnani and Quenneville [29] (included in the New Zealand Standard
530 draft [43]).

531 The designer should be able to evaluate possible brittle failure modes in connec-
532 tions, so he gets to avoid them in his design. The lack of knowledge shown by the
533 survey conducted within the COST Action [6] proves that design standards should in-
534 clude each failure mode in a clear and explicit way. It is expected that they will be
535 included in the main matter of the future version of the Eurocode 5 (see [6] for more

536 information). This work is a first step to provide background information for its de-
537 velopment. Further future works will provide insight into each one of the different
538 failure modes, in order to assess the influence of geometrical parameters in this type of
539 failures.

540 **Acknowledgement**

541 Both authors would like to acknowledge the contribution of the COST Action
542 FP1402, supported by COST (European Cooperation in Science and Technology), for
543 the development of this work, especially the related discussion within the Working
544 Group 3 "Connections". Authors wish to place on record their thanks to the mem-
545 bers of the Working Group CEN/TC250/SC5/WG5 "Connections", within the Working
546 Commission of the Eurocode 5, for their valuable comments.

547 The second author is supported by a PhD fellowship from the Programa de Becas
548 FPU del Ministerio de Educación y Ciencia (Spain) under the grant number FPU15/03413.
549 He would also like to thank the Asociación de Amigos of the University of Navarra for
550 their help with a fellowship in early stages of this research.

551 **References**

- 552 [1] E. Frühwald, E. Serrano, T. Toratti, A. Emilsson, S. Thelandersson, Design of
553 safe timber structures – How can we learn from structural failures in concrete ,
554 steel and timber ? Design of safe timber structures – Report TVBK-3053, Tech.
555 Rep., Lund University, 2007.
- 556 [2] E. Frühwald, Analysis of structural failures in timber structures: Typical causes
557 for failure and failure modes, *Engineering Structures* 33 (11) (2011) 2978–2982,
558 ISSN 01410296, doi:10.1016/j.engstruct.2011.02.045.
- 559 [3] Eurocode 5, CEN:EN 1995-1-1:2004 - Eurocode 5: Design of timber structures
560 - Part 1-1: General - Common rules and rules for buildings, Comité Européen de
561 Normalisation, 2004.
- 562 [4] K. W. Johansen, Theory of Timber Connections, *International Association of*
563 *Bridge and Structural Engineering* 9 (1949) 249–262, doi:10.5169/seals-9703.
- 564 [5] Biger JP, Bocquet JF, Racher P, Testing and designing the joints for the pavil-
565 ion of Utopia, in: *World Conference on Timber Engineering (WCTE)*, Whistler,
566 Canada,, Paper 4–3–3, 2000.
- 567 [6] M. Stepinac, J. M. Cabrero, K. Ranasinghe, M. Kleiber, Reorganization of the
568 Connections Chapter of the Eurocode 5, *Engineering Structures* (this issue).
- 569 [7] COST Action FP1402 "Basis of Structural Timber Design" - from research to
570 standards, Webpage, URL <https://www.costfp1402.tum.de/en/>, 2017.
- 571 [8] M. Hansson, H. J. Larsen, Recent failures in glulam structures and their
572 causes, *Engineering Failure Analysis* 12 (5 SPEC. ISS.) (2005) 808–818, ISSN
573 13506307.

- 574 [9] ENV 1995-1-1:1993. Eurocode 5, Design of Timber Structures, Part 1-1: General
575 Rules and Rules for Buildings., Comité Européen de Normalisation, 1993.
- 576 [10] A. Ranta-Maunus, A. Kevarinmäki, Reliability of timber structures. Theory and
577 dowel-type connection failures, in: CIB-W18 Timber Structures, Colorado, USA,
578 Paper 36-7-11, 2003.
- 579 [11] P. Racher, STEP/Eurofortech, Timber Engineering Volume, vol. 1, chap. Lecture
580 C1. Mechanical timber joints - General, Centrum Hout, Almere, The Netherlands,
581 1994.
- 582 [12] H. Fahlbusch, Ein Beitrag zur Frage der Tragfaehigkeit von Bolzen in Holz bei
583 statischer Belastung, Ph.D. thesis, Technische Hochschule Braunschweig, 1949.
- 584 [13] H. Blaß, Load distribution in nailed joints, in: CIB-W18 Timber structures, Lis-
585 bon, Portugal, Paper 23-7-2, 1990.
- 586 [14] W. Nozynski, Investigation of the effect of number of nails in a joint on its load
587 carrying ability, in: CIB W-18 Timber Structures, Otaniemi, Finland, Paper 13-
588 7-2, 1980.
- 589 [15] E. Gehri, Design of joints and frame corners using dowel-type fasteners, in: CIB-
590 W18 Timber structures,, Bordeaux, France, Paper 29-7-6, 1996.
- 591 [16] A. J. Jorissen, Double shear timber connections with dowel type fasteners, Ph.D.
592 thesis, TU Delft, 1998.
- 593 [17] M. Yasumura, T. Murota, H. Nakai, Ultimate properties of bolted joints in glued-
594 laminated timber, in: CIB-W18 Timber structures, Dublin, Ireland., Paper 20-7-
595 3, 1987.
- 596 [18] G. Steck, Effectiveness of multiple fastener joints according to national codes and
597 Eurocode 5 draft, in: CIB W-18 Timber Structures, Florence, Italy, Paper 19-7-3,
598 1986.
- 599 [19] I. Smith, G. Steck, Influence of number of rows of fasteners or connectors upon
600 the ultimate capacity of axially loaded timber joints, in: CIB W-18 Timber Struc-
601 tures, Beit Oren, Israel, Paper 18-7-3, 1985.
- 602 [20] A. Kevarinmäki, STEP/Eurofortech, Timber Engineering Volume, vol. 2, chap.
603 Lecture E6. Trusses made from laminated veneer lumber, Centrum Hout, Almere,
604 The Netherlands, 1995.
- 605 [21] R. Jockwer, Impact of varying material properties and geometrical parameters on
606 the reliability of shear connections with dowel type fasteners, in: International
607 Network on Timber Engineering Research (INTER), vol. 1052, Graz, Austria,
608 Paper 49-7-2, 2016.
- 609 [22] A. Hanhijärvi, A. Kevarinmäki, VTT publications 677: Timber Failure Mecha-
610 nisms in High-Capacity Dowelled Connections of Timber to Steel, VTT, Espoo,
611 ISBN 9789513870904, 2008.

- 612 [23] P. Quenneville, Predicting the failure modes and strength of brittle bolted con-
613 nections, in: Proceedings of the 5th World Conference on Timber Engineering
614 (WCTE), vol. 2, Montreux, Switzerland, 137–144, 1998.
- 615 [24] M. Mohammad, P. Quenneville, Behaviour of wood-steel-wood bolted glulam
616 connections, in: CIB-W18 Timber Structures, Graz, Austria, Paper 32–7–1, 1999.
- 617 [25] H. Johnsson, L. Stehn, Plug shear failure in nailed timber connections, *Holz als*
618 *Roh- und Werkstoff* (2004) 455–464 ISSN 0018-3768.
- 619 [26] H. Johnsson, G. Parida, Prediction model for the load-carrying capacity of nailed
620 timber joints subjected to plug shear, *Materials and Structures* 46 (12) (2013)
621 1973–1985, ISSN 1359-5997, doi:10.1617/s11527-013-0030-8.
- 622 [27] R. Foschi, J. Longworth, Analysis and design of griplam nailed connections, *J*
623 *Struct Div* 101 (12) (1975) 2537–2555.
- 624 [28] J. Kangas, J. Vesa, Design on timber capacity in nailed steel-to-timber joints, in:
625 CIB-W18 Timber Structures, Savonlinna, Finland, Paper 31–7–4, 1998.
- 626 [29] P. Zarnani, P. Quenneville, Group Tear-Out in Small-Dowel-Type Timber Con-
627 nections: Brittle and Mixed Failure Modes of Multinail Joints, *Journal of Struc-*
628 *tural Engineering* 141 (2) (2014) 4014110, ISSN 0733-9445, doi:10.1061/(asce)
629 st.1943-541x.0001053.
- 630 [30] P. Zarnani, P. Quenneville, Strength of timber connections under potential failure
631 modes: An improved design procedure, *Construction and Building Materials* 60
632 (2014) 81–90, ISSN 09500618, doi:10.1016/j.conbuildmat.2014.02.049.
- 633 [31] P. Zarnani, P. Quenneville, Wood Block Tear-Out Resistance and Failure Modes
634 of Timber Rivet Connections: A Stiffness-Based Approach, *Journal of Structural*
635 *Engineering* 140 (2) (2014) 04013055, ISSN 0733-9445, doi:10.1061/(ASCE)ST.
636 1943-541X.0000840.
- 637 [32] P. Zarnani, Load-Carrying Capacity and Failure Mode Analysis of Timber Rivet
638 Connections, Ph.D. thesis, University of Auckland, 2013.
- 639 [33] M. Marjerrison, P. Quenneville, Model for the predictions of the ductile and brittle
640 failure modes (parallel-to-grain) of timber rivet connections, in: CIB-W18
641 Timber Structures, Bled, Slovenia, Paper 40–7–6, 2007.
- 642 [34] A. J. Jorissen, Multiple fastener timber connections with dowel type fasteners, in:
643 CIB-W18 Timber Structures, Vancouver, Canada, Paper 30–7–5, 1997.
- 644 [35] J. L. Jensen, P. Quenneville, Fracture mechanics analysis of row shear failure
645 in dowelled timber connections., *Wood Science and Technology* 44 (4) (2009)
646 639–653, ISSN 00437719, doi:10.1007/s00226-009-0295-9.
- 647 [36] J. L. Jensen, P. Quenneville, Fracture mechanics analysis of row shear failure in
648 dowelled timber connections: asymmetric case, *Materials and Structures* 44 (4)
649 (2010) 351–360, doi:10.1617/s11527-010-9631-7.

- 650 [37] J. L. Jensen, P. Quenneville, Experimental investigations on row shear and splitting
651 in bolted connections, *Construction and Building Materials* 25 (5) (2011)
652 2420–2425, ISSN 09500618, doi:10.1016/j.conbuildmat.2010.11.050.
- 653 [38] CSA Standard. O86-09. Engineering design in wood, Canadian Standards Association,
654 2009.
- 655 [39] P. Quenneville, M. Mohammad, On the Failure Modes and Strength of Steel-
656 Wood-Steel Bolted Timber Connections Loaded Parallel to Grain, *Canadian Journal*
657 *of Civil Engineering* 27 (4) (2000) 761–773.
- 658 [40] M. Mohammad, P. Quenneville, Bolted wood-steel and wood-steel-wood connections:
659 verification of a new design approach, *Canadian Journal of Civil Engineering*
660 28 (2) (2001) 254–263, ISSN 0315-1468, doi:10.1139/100-105.
- 661 [41] M. Bickerdike, P. Quenneville, Predicting the row shear failure mode in parallel-
662 to-grain bolted connections, 9th World Conference on Timber Engineering 2006,
663 WCTE 2006 2 (2006) 1511–1518.
- 664 [42] P. Quenneville, I. Smith, A. Aziz, M. Snow, I. H. Chui, Generalised Canadian
665 approach for design of connections with dowel fasteners, in: *CIB-W18 Timber*
666 *Structures*, Florence, Italy, Paper 39–7–6, 2006.
- 667 [43] New Zealand Standard draft, specific amendments to AS 1720.1–2010, Unpub-
668 lished, 2017.
- 669 [44] A. Hanhijärvi, A. Kevarinmäki, Design method against timber failure mecha-
670 nisms of dowelled steel-to-timber connections, in: *CIB-W18 Timber Structures*,
671 Bled, Slovenia, Paper 40–7–3, 2007.
- 672 [45] S. A. L. Novis, J. Jacks, P. Quenneville, Predicting the resistance and displace-
673 ment of timber bolted connections, in: *World Conference on Timber Engineering*
674 *(WCTE 2016)*, Vienna, Austria, 2016.
- 675 [46] P. Zarnani, P. Quenneville, Design Procedure to Determine the Capacity of Tim-
676 ber Connections under Potential Brittle , Mixed and Ductile Failure Modes, in:
677 *CIB-W18 Timber Structure*, August, Paper 46–7–3, 2013.
- 678 [47] J. Sjödin, C.-J. Johansson, Influence of initial moisture induced stresses in multi-
679 ple steel-to-timber dowel joints, *Holz als Roh- und Werkstoff* 65 (1) (2006) 71–
680 77, ISSN 0018-3768.
- 681 [48] R. Jockwer, G. Fink, J. Köhler, Assessment of existing safety formats for timber-
682 connections - How probabilistic approaches can influence connection design in
683 timber engineering, in: *Proc. of the COST Action FP1402 at Graz University of*
684 *Technology*, vol. 1, Graz, Austria, 16–31, 2017.
- 685 [49] M. Schmid, Anwendung der Bruchmechanik auf Verbindungen mit Holz, Ph.D.
686 thesis, Universität Karlsruhe, Germany, 2002.

- 687 [50] J. Jensen, U. Girhammar, P. Quenneville, Brittle failure in timber connections
688 loaded parallel to the grain, *Proceedings of the Institution of Civil Engineers:*
689 *Structures and Buildings* 168 (10), ISSN 17517702 09650911, doi:10.1680/stbu.
690 14.00108.
- 691 [51] O. D. Volkersen, Die Nietkraftverteilung in zugbeanspruchten Nietverbindungen
692 mit konstanten Laschenquerschnitten, *Luftfahrtforschung* 35 (1938) 4–47.
- 693 [52] I. Smith, E. Landis, M. Gong, *Fracture and Fatigue in Wood*, Wiley, ISBN 0-471-
694 48708-2, 2003.
- 695 [53] M. Schmid, H. J. Blaß, R. P. M. Frasson, Effect of Distances , Spacing and Num-
696 ber of Dowels in a Row on the Load Carrying Capacity of Connections with Dow-
697 els Failing by Splitting, in: *CIB-W18 Timber Structures*, Kyoto, Paper 35–7–7,
698 2002.
- 699 [54] R. Jockwer, Structural behaviour of glued laminated timber beams with unrein-
700 forced and reinforced notches, Ph.D. thesis, IBK ETH Zurich, 2014.
- 701 [55] D. C. Stahl, R. W. Wolfe, M. Begel, Simplified analysis of timber rivet connec-
702 tions, *Journal of Structural Engineering* 130 (August) (2004) 1272–1279, ISSN
703 0733-9445, doi:10.1061/(ASCE)0733-9445(2004)130:8(1272).
- 704 [56] J.-F. Bocquet, C. Barthram, A. Pineur, L block failure of dowelled connections
705 subject to bending reinforced with threaded rods, in: *CIB-W18 Timber structures*,
706 Växjö, Sweden, Paper 45–7–3, 2012.
- 707 [57] B. Iraola, Simulación del Comportamiento Mecánico de la Madera en Uniones
708 Estructurales y su Aplicación mediante Modelos Tridimensionales de Elementos
709 Finitos, Ph.D. thesis, Universidad de Navarra, 2016.
- 710 [58] EN 14358:2016. Timber structures — Calculation and verification of characteris-
711 tic values, CEN, 2016.
- 712 [59] Council of Standards Australia (Ed.), AS/NZS 1328: 1998. Glued laminated
713 structural timber, 1998.
- 714 [60] EN 338:2016. Structural timber. Strength classes, CEN, 2016.
- 715 [61] Certificate. Kerto-S and LKerto-Q Structural laminated veneer lumber. Date of
716 issue March 24, 2004. Updated May 17,2016, Tech. Rep. 184/03, VTT Expert
717 Services Ltd., 2016.
- 718 [62] Joint Committee on Structural Safety (Ed.), JCSS Probabilistic Model Code,
719 chap. 3.5. Properties of Timber, JCSS, 2006.
- 720 [63] R. Jockwer, G. Fink, Material properties according to JCCS Probabilistic model
721 code, MatLab script, 2017.
- 722 [64] R. Jockwer, G. Fink, K. J., Assessment of the failure behaviour and reliability of
723 timber connections, *Engineering Structures* (this issue).

- 724 [65] Joint Committee on Structural Safety (Ed.), JCSS Probabilistic Model Code,
725 chap. 3.2. Structural steel, JCSS, 2006.
- 726 [66] E. W. Steyerberg, A. J. Vickers, N. R. Cook, T. Gerds, M. Gonen, N. Obu-
727 chowski, M. J. Pencina, M. W. Kattan, Assessing the Performance of Pre-
728 diction Models, *Epidemiology* 21 (1) (2010) 128–138, ISSN 1044-3983, doi:
729 10.1097/EDE.0b013e3181c30fb2.
- 730 [67] A. Golbraikh, A. Tropsha, Beware of q^2 !, *Journal of Molecular Graph-*
731 *ics and Modelling* 20 (4) (2002) 269–276, ISSN 1093-3263, doi:10.1016/
732 S1093-3263(01)00123-1.
- 733 [68] D. L. Alexander, A. Tropsha, D. A. Winkler, Beware of R^2 : Simple, Unambiguous
734 Assessment of the Prediction Accuracy of QSAR and QSPR Models, *Journal of*
735 *Chemical Information and Modeling* 55 (7) (2015) 1316–1322, ISSN 15205142,
736 doi:10.1021/acs.jcim.5b00206.
- 737 [69] K. Roy, P. Chakraborty, I. Mitra, P. K. Ojha, S. Kar, R. N. Das, Some case stud-
738 ies on application of " r_m^2 " metrics for judging quality of quantitative structure-
739 activity relationship predictions: Emphasis on scaling of response data, *Journal*
740 *of Computational Chemistry* 34 (12) (2013) 1071–1082, ISSN 01928651, doi:
741 10.1002/jcc.23231.
- 742 [70] K. Roy, R. N. Das, P. Ambure, R. B. Aher, Be aware of error measures. Further
743 studies on validation of predictive QSAR models, *Chemometrics and Intelligent*
744 *Laboratory Systems* 152 (2016) 18–33, ISSN 18733239, doi:10.1016/j.chemolab.
745 2016.01.008.
- 746 [71] P. Gramatica, A. Sangion, A Historical Excursus on the Statistical Validation Pa-
747 rameters for QSAR Models: A Clarification Concerning Metrics and Terminol-
748 ogy, *Journal of Chemical Information and Modeling* 56 (6) (2016) 1127–1131,
749 ISSN 15205142, doi:10.1021/acs.jcim.6b00088.
- 750 [72] N. Chirico, P. Gramatica, Real external predictivity of QSAR models. Part 2.
751 New intercomparable thresholds for different validation criteria and the need for
752 scatter plot inspection, *Journal of Chemical Information and Modeling* 52 (8)
753 (2012) 2044–2058, ISSN 15499596, doi:10.1021/ci300084j.
- 754 [73] N. Chirico, P. Gramatica, Real external predictivity of QSAR models: How to
755 evaluate It? Comparison of different validation criteria and proposal of using the
756 concordance correlation coefficient, *Journal of Chemical Information and Mod-*
757 *eling* 51 (9) (2011) 2320–2335, ISSN 15499596, doi:10.1021/ci200211n.
- 758 [74] P. Quenneville, Predicting the Failure Modes and Strength of Brittle Bolted Con-
759 nections, in: *World Conference in Timber Engineering*, Montreux, Switzerland,
760 1998.
- 761 [75] K. Roy, I. Mitra, S. Kar, P. K. Ojha, R. N. Das, H. Kabir, Comparative studies
762 on some metrics for external validation of QSPR models, *Journal of Chemical*

763 Information and Modeling 52 (2) (2012) 396–408, ISSN 15499596, doi:10.1021/
764 ci200520g.

765 [76] P. K. Ojha, I. Mitra, R. N. Das, K. Roy, Further exploring r_m^2 metrics for valida-
766 tion of QSPR models, Chemometrics and Intelligent Laboratory Systems 107 (1)
767 (2011) 194–205, ISSN 01697439, doi:10.1016/j.chemolab.2011.03.011.

768 [77] I. Mitra, P. P. Roy, S. Kar, P. K. Ojha, K. Roy, On further application of r_m^2 as a
769 metric for validation of QSAR models, Journal of Chemometrics 24 (1) (2010)
770 22–33, ISSN 08869383, doi:10.1002/cem.1268.

771 **Nomenclature**

772 **Greek Symbols**

773 α Friction angle between the fastener and the timber in the hole

774 α_t Tensile stress coefficient [27]

775 β_t, β_s Stress coefficients (tensile and shear) based on nail spacing [27]

776 β_p Ratio of the perpendicular-to-grain wedging force to the parallel-to-grain fas-
777 tener load

778 γ_h Stress coefficient depending on nail penetration [27]

779 Γ_i Additional expressions related to the relative stiffness of each failure plane
780 [43, 29–31, 46]

781 Φ Factor function of fracture energy, location and geometry [35]

782 **Lower cases**

783 a_1 Spacing between columns of fasteners

784 a_2 Spacing between rows of fasteners

785 a_3 Distance to the parallel-to-grain edge

786 a_4 Distance to the perpendicular-to-grain edge

787 $a_{L,min}$ Minimum of a_1 and a_3

788 b Width of the wood member

789 b_c Width of the connection

790 b_{net} Net width of the connection

791 c Rank correlation coefficient [68]

792 d Fastener diameter

793	d_r	Rivet short diameter
794	\bar{f}	Average predicted values
795	f_i	Predicted values
796	$f_{h,0}$	Embedment strength in the parallel-to-grain direction
797	$f_{r,h,0}$	Embedment strength for rivets in the parallel-to-grain direction
798	$f_{t,90}$	Tensile strength parallel-to-grain
799	$f_{t,90}$	Tensile strength perpendicular-to-grain
800	f_v	Shear strength
801	f_y	Yield strength of the fastener
802	k_{con}	Factor of stress concentration [22]
803	k_{ef}	Geometric coefficient for determining the n_{ef} of nails in Eurocode 5 [3]
804	$k_{t,cnctr}, k_{v,cnctr}$	Stress concentration factors depending on the timber product [22]
805	k_v	Factor depending on the load distribution [22]
806	k_{int}	Interaction factor in Hanhijärvi and Kevarinmäki [22]
807	ℓ	Penetration length of a small fastener in the wood
808	m	Slope of a linear fit passing through the origin
809	n	Number of tests
810	n_c	Number of fastener columns of the connection
811	n_{ef}	Number of effective fastener columns of the connection
812	n_r	Number of fastener rows of the connection
813	n_s	Number of shear planes of the connection
814	n_w	Number of wood members of the connection
815	r_m^2	Coefficient correlation based on the slope of different fitting procedures [75–
816		77]
817	$s_{t,90,i}$	Geometric parameters for splitting [22]
818	t	Thickness of the wood member
819	t_{ef}	Effective thickness of the connection
820	t_p	Steel plate thickness

821	\bar{y}	Average of experimental values
822	y_i	Experimental values
823	Upper cases	
824	CCC	Concordance correlation coefficient, defined in (3) [71, 73, 72]
825	E_0	Modulus of elasticity in the parallel-to-grain direction
826	G	Modulus of rigidity
827	G_f	Fracture energy value
828	J_r	Factor depending on the number of rows[23, 40]
829	K_H, K_B, K_L	Stiffness of head, bottom, and lateral planes [43, 29–31, 46]
830	K_t, K_s	Coefficients (tensile and shear) depending on the n_c and n_r [27]
831	k_{LS}	Factor depending on the load distribution along the fastener[43]
832	L_c	Length of the connection
833	L_{net}	Net length of the connection
834	$M_{r,y}$	Rivet yield moment.
835	M_y	Fastener yield moment.
836	MRE	Mean relative error, defined in (4)
837	Q^2	Coefficient of correlation defined in (2) [66, 73]
838	R_5	Over-prediction coefficient when characteristic properties values are applied
839	SD	Standard deviation of the mean relative error
840	X_s, X_t	Parameters function of the timber product [43]